



## DAVINCI

### Pixel Scales and Sensitivities

December 9, 2009 Revised April 10, 2010

## INTRODUCTION

This document describes the proposed pixel scale for the DAVINCI imager and gives a rationale for the selected scales. Because the sensitivity of the instrument is also related to the choice of pixel scale (all other things being equal), an analysis of the expected point source sensitivities over the wavelength range of 0.7 to 2.4  $\mu\text{m}$  is presented. A future update to this document will include discussion of the sensitivities for extended objects.

The discussion in this document is based on the current DAVINCI optical design and the DAVINCI background and zero point estimates presented in Adkins and McGrath (2010).

## DETECTOR PIXEL SCALES

As described in Kupke (2009) the NGAO science relay will offer an unvignetted field of view (FOV) covering 40" diameter. We assume that the NGAO relay offers diffraction limited performance over the full NGAO wavelength range. We also assume that while the Strehl provided by adaptive optics correction will diminish at the shorter wavelengths, the core of the PSF is still equal to the diffraction limited image size even for a comparatively low Strehl.

The discussion of what detector pixel scale or scales should be provided is based on the following considerations:

1. **Spatial sampling:** the imager should provide at least 2 pixels sampling across the FWHM of the Airy disk ( $\sim\lambda/D$ ).
2. **Optimal sampling:** the optimal sampling will require consideration of the signal to noise ratio (SNR) and how the image will be used. In general, when SNR is high, more than two pixel sampling is beneficial, especially for PSF determination, astrometry, and photometry.
3. **FOV:** the FOVs required by the key science drivers range from 4" to 10", with larger FOVs of 15" or more desired for certain science drivers (see Adkins et al. 2009). The minimum FOV should be one that meets as many of the science requirements as possible without becoming a driver on instrument cost (cost will mainly be driven by the size of the clear apertures for the lenses or mirrors in the optical system and the required detector size). The FOV should also be chosen to take full advantage of the field available from the AO system, keeping in mind the fact that Strehl will fall somewhat as the field radius is increased. The FOV should not exceed the FOV of the science relay by any significant amount or expensive detector pixels will go unused.
4. **Background:** the sky background levels in the near-IR, combined with thermal emission from the telescope and AO system, especially in the K-band result in pixels with larger on sky area (a coarser pixel scale) becoming background limited more quickly than pixels with a smaller on sky area.
5. **Read noise and dark current:** smaller pixels will increase the read noise and dark current noise contribution for a given extended object size.



6. **Imager performance, complexity, and cost:** for reasons of complexity, optical performance, and cost it is desirable to have only one imager spatial sampling scale.
7. **Detector size and pixel dimensions:** the NGAO imager will use a 4096 x 4096 pixel IR focal plane array with 15  $\mu\text{m}$  pixels (the Hawaii-4RG).

Given a square detector, the square area that will fall entirely within a 40" FOV is 28.28" x 28.28". Given a 4096 x 4096 pixel detector, the corresponding pixel scale is 7 mas. A second candidate is an 8 mas scale, which provides a FOV of 32.8" x 32.8". With the 8 mas pixel scale there is a loss of ~3% of the detector area due to vignetting at the corners of the detector as shown in Figure 1.

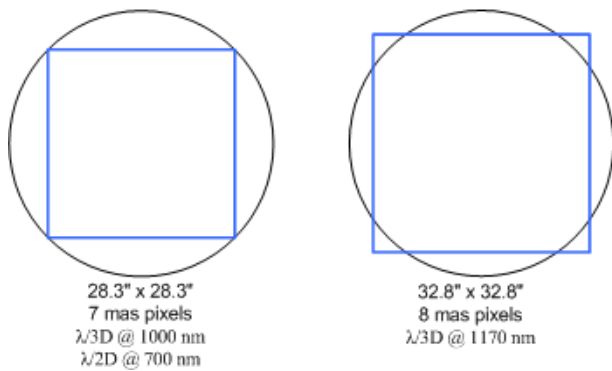


**Figure 1: Candidate imager FOVs (blue squares) overlaid on the NGAO science FOV (black circles)**

Table 1 lists the cut-on and cut-off wavelengths for the 6 DAVINCI photometric passbands. The sampling obtained in each passband for pixel scales of 7 and 8 mas is illustrated in Figure 2. A more detailed listing of spatial sampling in terms of  $\lambda/D$  for each waveband is provided in the appendix (Table 9).

DAVINCI photometric passband	Wavelength, nm
K band cut-off	2370
K band cut-on	2030
H band cut-off	1780
H band cut-on	1490
J band cut-off	1330
J band cut-on	1170
Y band cut-off	1070
Y band cut-on	970
z band cut-off	922
z band cut-on	818
I band cut-off	853
I band cut-on	700

**Table 1: DAVINCI photometric passbands**

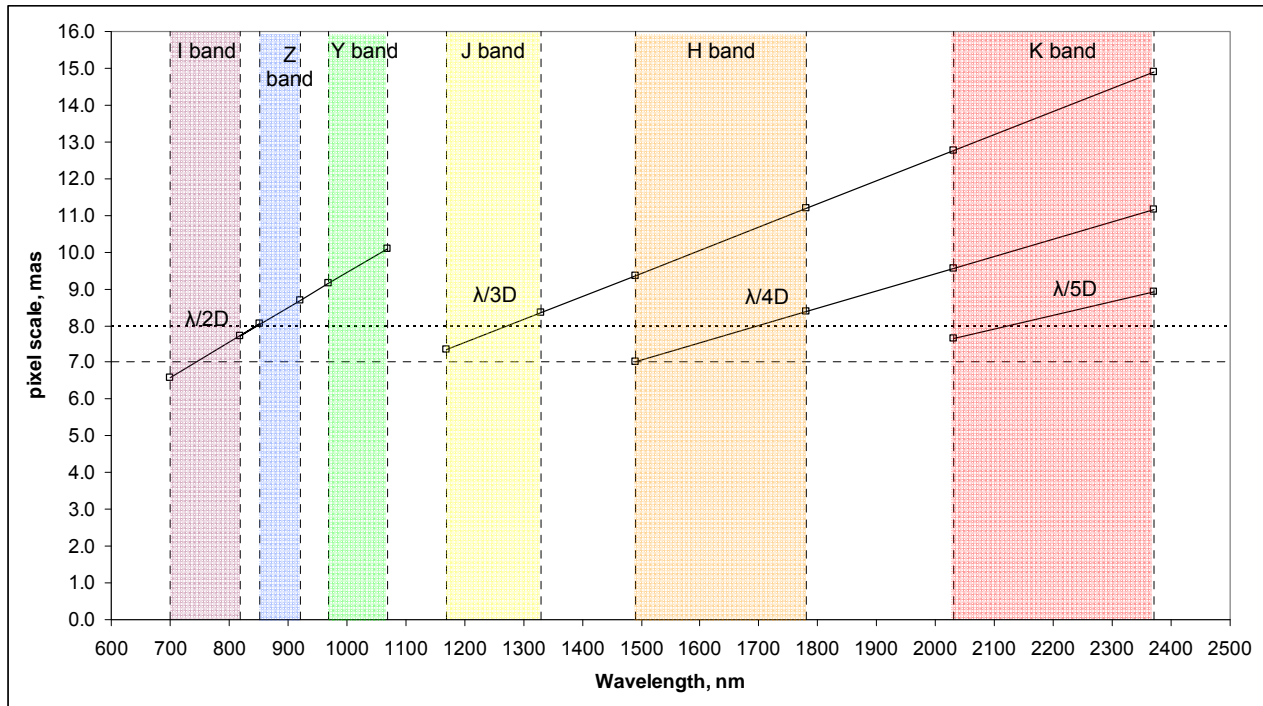


**Figure 2: DAVINCI photometric wavelength bands and spatial sampling**

From Figure 2 we can see that a 7 mas pixel scale would provide >2 pixel sampling down to near the I band cut-on wavelength, >2 pixel sampling in the Z and Y bands, >3 pixel sampling in the J band,  $\geq 4$  pixel sampling in H, and > 5 pixel sampling in K band. An 8 mas pixel scale would provide 1 to 2 pixel sampling in I band, >2 pixel sampling in the Z and Y bands, 2 to 3 pixel sampling in the J band, 3 or more pixel sampling in H, and 4 to 5 pixel sampling in K band. The benefit of the 8 mas pixel scale would be an increased FOV.

### Limits on Imager Performance due to the AO System

The off-axis performance of the AO system will be limited by anisoplanatic effects, although the central portion of the field will be much more uniformly corrected due to the use of tomographic wavefront reconstruction. An example of the predicted Strehl for field diameters up to 34" is shown in Figure 10 of Dekany et al. (2009).

The NGAO AO relays use off-axis parabolas (OAPs) to collimate the light and to produce a pupil at each deformable mirror (DM). This pupil is located off the optical axis of the OAP collimator, resulting in aberration of the pupil image on the DM (Bauman, 2009). As Bauman shows, for a given field size a smaller DM results in more severe aberrations, the effect of which is to introduce another form of anisoplanatism. This effect will be quantified in an end to end analysis of the combined performance of the NGAO system including DAVINCI.



The overall pupil image from the AO system exhibits field dependent pupil image shifts and pupil distortions both of which impact the quality of the background suppression obtained from DAVINCI's cold stop. In the current DAVINCI optical design the pupil image at the instrument's cold stop is formed using the first off-axis parabola in an OAP pair that forms the instrument's internal intermediate focal plane. This approach compensates the pupil image and improves cold stop performance.

Spatial distortion of the image at the detector focal plane is an important issue for astrometry. The DAVINCI optical design goal is to keep distortion to <2% over the full unvignetted area of the detector (Adkins, 2009b). In the current DAVINCI optical design the distortion present is simple barrel distortion with a maximum of 1% over the entire FOV. This level of distortion should be able to be calibrated out using a precision reference grid or other focal plane spatial calibrator.

### **Detector Pixel Scale and Sensitivity**

As noted earlier, adopting a single detector pixel scale dictated by the finest pixel scale needed to properly sample the diffraction limit at the shortest wavelength of interest will result in oversampling at longer wavelengths. This can be expected to have an impact on sensitivity since having more pixels across the FWHM will increase the dark current noise and read noise in the image. At the same time, smaller pixels will see less sky and system background, increasing the permissible exposure time without approaching detector saturation. In the discussion of sensitivities found in the next section of this document we include consideration of the impact of a fixed detector plate scale on performance at longer wavelengths.

### **SENSITIVITY**

To predict the sensitivity of the NGAO science imager we need to determine quantities for the total signal and the noise in that signal. The total signal,  $S$ , in electrons, is described by equation 1. Note that for all calculations we assume a gain of 1 DN per electron.

$$S = (P_{object} \times QE \times N \times t \times Strehl) + (P_{background} \times QE \times N \times t \times Pixels) + (D \times N \times t \times Pixels)$$

where :

$P_{object}$  = object photons/s reaching the detector

$QE$  = the manufacturer's specified detective quantum efficiency,

i.e. a QE of 1 means each interacting photon generates 1 electron of signal

$N$  = number of exposures

$t$  = exposure time in seconds

$Strehl$  = Strehl provided by the AO correction

$P_{sky}$  = sky photons/s/pixel reaching the detector

$P_{background}$  = total background photons/s/pixel (Sky + telescope +AO) reaching the detector

$D$  = dark current signal in electrons/pixel/s

$Pixels$  = the number of image pixels

(1)



Next Generation Adaptive Optics  
**DAVINCI Imager Plate Scales and Sensitivities**  
 December 9, 2009 Revised April 10, 2010

---

The predicted average Strehl in each of the AO system passbands based on 170 nm residual wavefront error is computed as the average at the cut-on and cut-off wavelength using the extended Marechal approximation as shown in equation 2 (Hardy, 1998, p. 115).

$$Strehl = e^{-(\sigma_p)^2}$$

where :

$$\sigma_p = 2 \times \pi \times \frac{wfe}{\lambda}$$
(2)

and :

$wfe$  = rms wavefront error in nm

$\lambda$  = wavelength in nm

The resulting Strehl in each passband is given in Table 2.

Passband	Ave. Strehl (170 nm wavefront error)
I band photometric	15%
Z band photometric	22%
Y band photometric	33%
J band photometric	39%
H band photometric	59%
K band photometric	79%

**Table 2: Predicted Strehl in each photometric passband**

If we assume perfect background subtraction then the total object signal  $S_{object}$  in electrons is described by equation 3.

$$S_{object} = P_{object} \times QE \times N \times t \times Strehl$$
(3)

The required aperture for a diffraction limited image is assumed to be that needed for a well compensated image (Hardy, 1998, p. 42), i.e. a diameter equal to  $\frac{2 \times \lambda}{D}$  where  $D$  is the diameter of the telescope aperture, and  $\lambda$  is the long wavelength cut-off in the passband of interest. Based on this assumption we determine the total number of pixels for a point source as shown in equation 4.

$$Pixels = \frac{\pi * \left(206265 * \frac{\lambda}{D}\right)^2}{\theta_{pixel}^2}$$

where :

$$\lambda = \text{wavelength in nm} \times 10^{-9}$$
(4)

$D$  = diameter of telescope aperture in m

$\theta_{pixel}$  = angular size of each pixel on the sky in arcseconds



Next Generation Adaptive Optics  
**DAVINCI Imager Plate Scales and Sensitivities**  
 December 9, 2009 Revised April 10, 2010

---

The noise in the signal is described by equation 5.

$$Noise = \sqrt{S_{object} + (P_{background} \times QE \times N \times t \times Pixels) + (D \times N \times t \times Pixels) + (Pixels \times N \times R^2)}$$

where: (5)

$R$  = rms read noise in electrons per pixel per read

The SNR is then given by equation 6.

$$SNR = \frac{S_{object}}{Noise} \times \sqrt{N}$$
(6)

To determine the object photons use flux densities for Vega as given in Tokunaga and Vacca (2005), Table 1, and estimates for the NGAO I, Z, and Y bands as discussed in appendix A of Adkins and McGrath (2010).

The object flux  $P_{object}$  for a given magnitude star ( $M$ ) in a given passband in units of photons/s is calculated using equation 7.

$$P_{object} = 10^{(-0.4 * M)} \times F_v \times P_F \times \frac{\Delta\lambda}{\lambda} \times A_{tel} \times T_{atm} \times T_{tel} \times T_{AO} \times T_{filter} \times T_{inst}$$

where :

$M$  = magnitude in a given passband  
 $F_v$  = flux in Janskys (from Tokunaga, 2005)  
 $P_F$  = conversion from Janskys to photons/s/m<sup>2</sup> where 1 Jansky = 1.51 × 10<sup>7</sup> photons/s/m<sup>2</sup>  
 $\frac{\Delta\lambda}{\lambda}$  = bandpass filter FWHM divided by the central wavelength of the filter (7)  
 $A_{tel}$  = collecting area of the telescope in m  
 $T_{atm}$  = transmission of the atmosphere at zenith  
 $T_{tel}$  = transmission of the telescope  
 $T_{AO}$  = transmission of the AO system  
 $T_{filter}$  = passband transmission of the selected filter  
 $T_{inst}$  = transmission of the instrument

For the initial set of calculations we assume an average value for atmospheric transmission, telescope transmission, and AO system transmission over each passband as shown in Tables 2 and 3 of Adkins and McGrath (2010) as well as the DAVINCI imager's zero point magnitudes  $m_z$  and the background in magnitudes per square arcsecond for each photometric passband, also in Adkins and McGrath.



### IMAGER PERFORMANCE PREDICTIONS

The imager performance predictions are based on the minimum acceptable values for a Hawaii-4RG (H4RG) IR FPA with a 2.5  $\mu\text{m}$  cut-off as described in Adkins (2009a). The relevant parameters for this analysis are summarized in Table 3.

Parameter	Goal Value	Notes
Dark Current	0.01 $e^-/s$	Median dark current of all imaging pixels
Charge Storage Capacity	100,000 $e^-$ /pixel	Array average number of electrons where the photon transfer curve first deviates from a straight line
Read Noise	15 $e^-$ /pixel	Per CDS read
Quantum Efficiency	0.80 0.75 0.70	970 to 2400 nm 850 to 970 nm 700 to 850 nm

**Table 3: Hawaii-4RG performance parameters**

### Effect of Pixel Scale on Performance

Equation 3 describes the number of pixels assuming a circular aperture for a given pixel scale. The corresponding area is constant for all pixel scales in a given passband and therefore the background contribution is constant for all pixel scales in that passband. The read noise clearly increases as the pixel scale becomes smaller due to the greater number of pixels that will be read out. Since the K band represents the largest diffraction limited image size, and also has the highest background levels due to thermal sources, we start the analysis of pixel scale using the K band.

The number of pixels in the circular aperture for pixel scales from 100 mas to 5 mas, along with the resulting total read noise contribution, assuming single CDS read noise of 15  $e^-$ /pixel/read, and read noise of 4  $e^-$ /pixel/read for 16 Fowler samples (performance recently demonstrated by H2RG detector testing in the MOSFIRE project, Kulas, 2010) is shown for the K band aperture size (0.076" diameter) in Table 4.

Pixel scale, mas	100	50	20	15	10	8	7	5
Number of pixels, K band	1.0	1.8	11.5	20.4	46.0	71.8	93.8	183.8
Total read noise, $e^-$ , single CDS	15.0	20.3	50.8	67.8	101.7	127.1	145.3	203.4
Total read noise, $e^-$ , 16 Fowler samples	4.0	5.4	13.6	18.1	27.1	33.9	38.7	54.2

**Table 4: Number of pixels and total read noise for the K band aperture size at various pixel scales**

As expected, a smaller pixel scale results in increased read noise. It should be noted that in the following performance analysis for point sources we ignore the fact that we actually have a square aperture with an integer number of pixels.



Next Generation Adaptive Optics  
**DAVINCI Imager Plate Scales and Sensitivities**  
 December 9, 2009 Revised April 10, 2010

*Point Source Limiting Magnitude*

Assuming perfect background subtraction, the point source limiting magnitudes for an SNR of 5 in one hour (four 900 s exposures) for the K band are shown in Table 5 and Figure 3.

Pixel scale, mas	100	50	20	15	10	8	7	5
K band magnitude	26.20	26.65	26.65	26.65	26.65	26.65	26.65	26.65

**Table 5: K band limiting magnitudes for an SNR of 5 in one hour**

Note that the assumption that the collection aperture cannot be less than 1 pixel in diameter penalizes the 100 mas pixel scale by increasing the area from the diffraction limited value of  $3.6 \text{ mas}^2$  to  $10 \text{ mas}^2$ , resulting in an increase in the sky background. There is essentially no difference in the sensitivity for pixel scales from 50 to 5 mas.

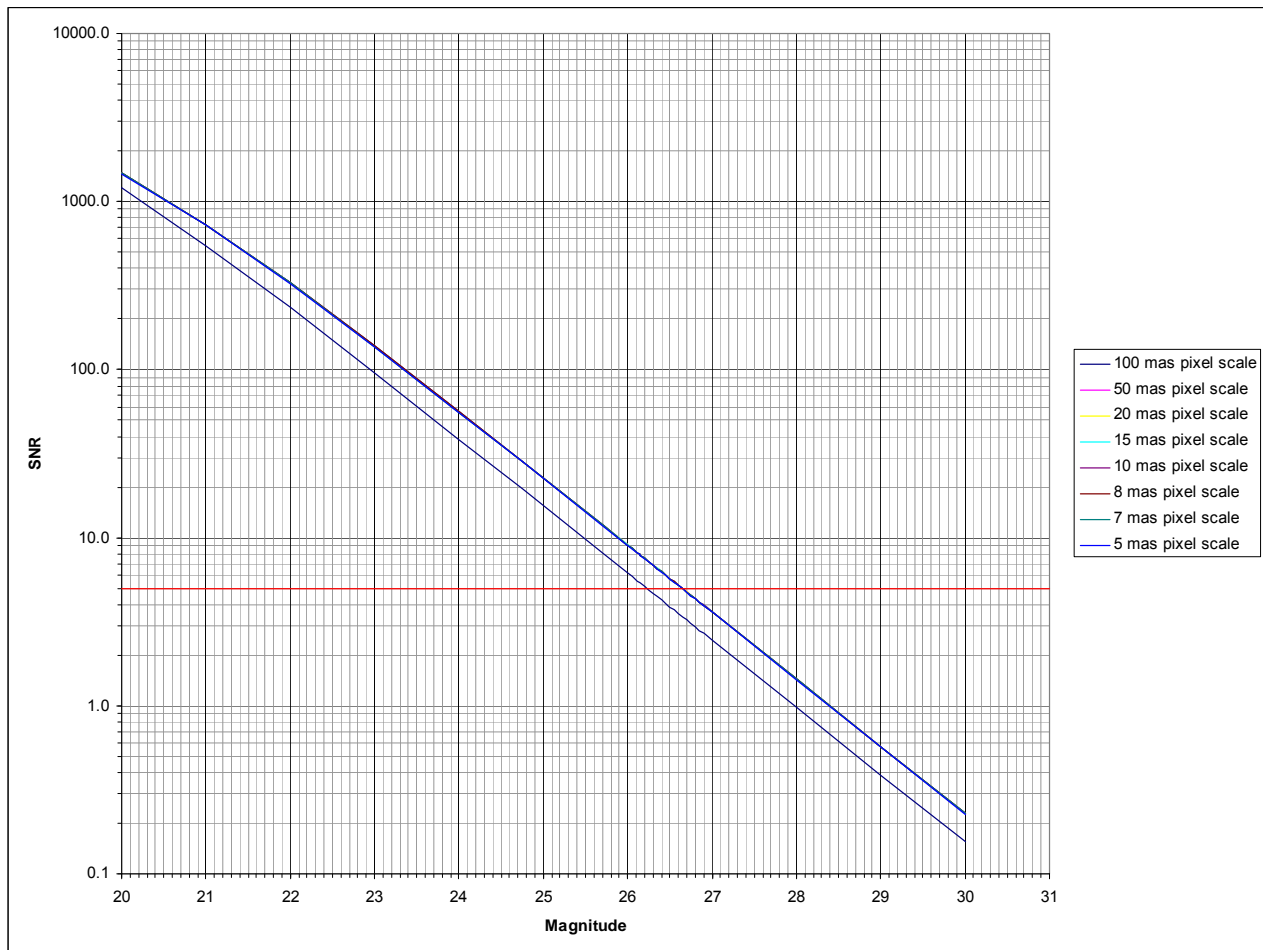


**Figure 3: K band limiting magnitudes vs. pixel scale for a 1 hour exposure**  
*An SNR of 5 is indicated by the red line.*



*Background Limited Exposure Times*

The SNR as a function of magnitude, assuming a background limited exposure, and an exposure including read noise was calculated for the 7, 8, and 10 mas pixel scales using exposure times from 10 to 1000 s. The result for the 8 mas pixel scale is shown in Figure 4. In the Figure the solid lines are the resulting SNR at each exposure time including read noise, and the dashed lines are the SNR for a background limited exposure. Where the lines are co-incident for a given exposure time the exposure has become background limited. This is achieved at  $\sim 280$  s with an SNR difference between the exposure with read noise and a background limited exposure of 1.1% for  $K = 27$ . The 10 mas pixel scale is about 0.1% better for the same magnitude, and the 7 mas pixel scale is about 0.1% worse.

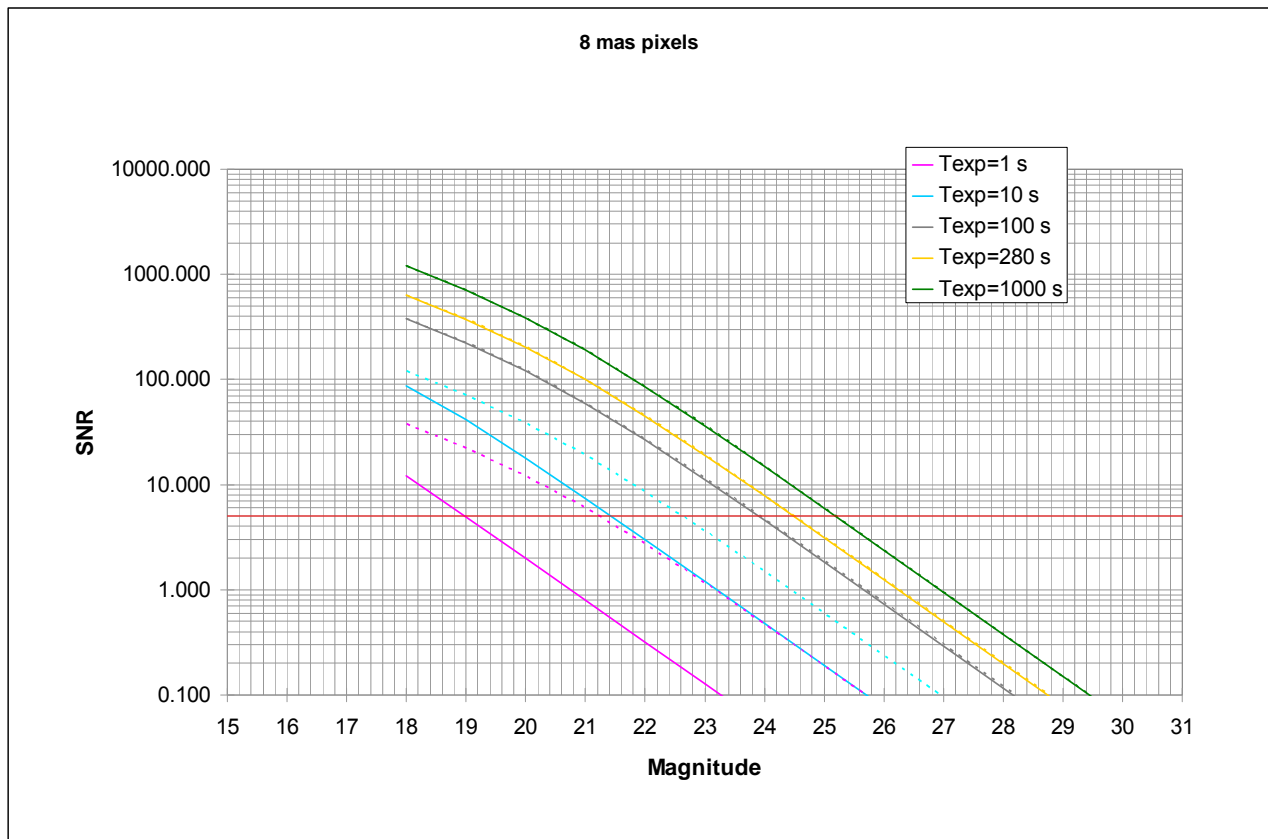


**Figure 4: SNR vs. K band magnitude for 1, 10, 100, 280 and 1000 s exposures and an 8 mas pixel scale**  
 An SNR of 5 is indicated by the red line. The dashed lines are for background limited conditions.

*Maximum Exposure Time*

Another consideration with respect to pixel scale is the maximum duration for a single exposure before a pixel is saturated. Smaller pixels allow a longer exposure for a given flux level, assuming a constant area on the sky. For the expected K band sky background magnitude of 14.78 per square arc second



Next Generation Adaptive Optics  
**DAVINCI Imager Plate Scales and Sensitivities**  
 December 9, 2009 Revised April 10, 2010

(Adkins & McGrath, 2010) the maximum time for a single exposure in K band to 50% of the detector’s full charge storage capacity at each of the pixel scales in Table 4 is shown in Figure 5.

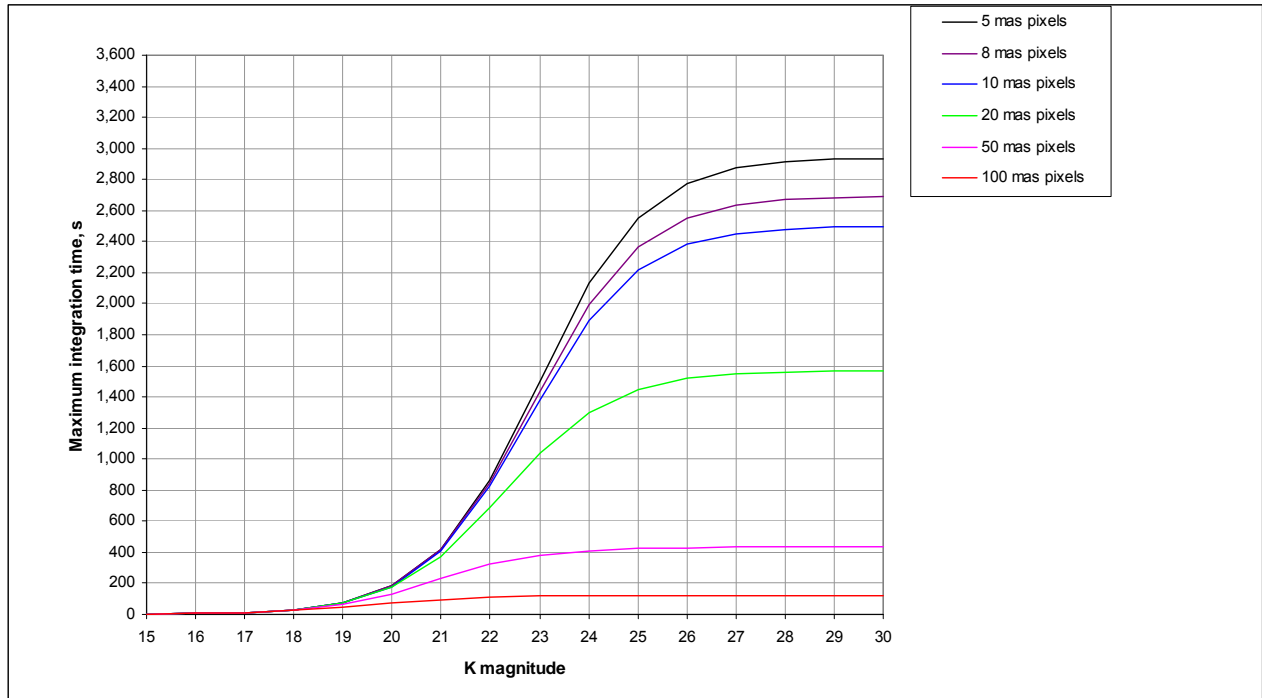


**Figure 5: Maximum exposure time (to 50% of full charge storage capacity) vs. K magnitude**

The maximum exposure time to 50% of the typical value for the H4RG detector’s maximum charge storage capacity of 100,000 e<sup>-</sup> is ~121 s for the 100 mas scale, and increases to ~2690 s for the 8 mas scale, and ~2780 s for the 7 mas scale.

**Performance Predictions for all Wavelengths**

The limiting magnitudes for each of the DAVINCI imaging passbands as a function of pixel scale are given in Table 6. The I and Z band values are based on four 120 s exposures, the Y through K band values are based on four 900 s exposures.

Pixel scale, mas	100	50	20	15	10	8	7	5
<b>I band magnitude</b>	27.30	27.90	28.35	28.20	27.90	27.90	27.70	27.60
<b>Z band magnitude</b>	27.25	27.95	28.35	28.20	27.95	27.80	27.70	27.40
<b>Y band magnitude</b>	26.75	27.50	27.95	27.95	27.95	27.95	27.95	27.90
<b>J band magnitude</b>	26.35	27.35	27.35	27.35	27.35	27.35	27.35	27.35
<b>H band magnitude</b>	25.70	26.40	26.40	26.40	26.40	26.40	26.40	26.40
<b>K band magnitude</b>	26.20	26.65	26.65	26.65	26.65	26.65	26.65	26.65

**Table 6: Limiting magnitudes for an SNR of 5**

The background limited exposure time for each of the imaging passbands with a point source magnitude of 27 are given in Table 7 for the 10, 8, and 7 mas pixel scales.



Pixel scale, mas	10	8	7
I band	4.7 h	6.7 h	7.8 h
Z band	3.9 h	5.6 h	6.7 h
Y band	1200 s	1800 s	2400 s
J band	360 s	560 s	720 s
H band	45 s	70 s	90 s
K band	200 s	280 s	400 s

**Table 7: Background limited exposure time in s**

The maximum exposure time to 50% of the typical value for the H4RG detector's maximum charge storage capacity of 100,000 e<sup>-</sup> are given in Table 8 for the 10, 8, and 7 mas pixel scales in each of the imaging passbands assuming a point source magnitude of 30.

Pixel scale, mas	10	8	7
I band	3120	3120	3120
Z band	3117	3118	3118
Y band	3007	3047	3064
J band	2770	2886	2940
H band	1520	1863	2057
K band	2500	2690	2780

**Table 8: Maximum exposure time in s to 50% of detector charge storage capacity**

## CONCLUSIONS

For the infrared bands the sky background is the dominant factor in the SNR as indicated by the relatively short exposure times required to reach a background limited exposure. This is also reflected in the limited impact on 5 $\sigma$  limiting magnitude for the range of pixel scales from 50 mas to 5 mas as shown in Table 6. This suggests there is no compelling sensitivity argument to guide the selection of pixel scale in the range of choices that address the diffraction limited sampling requirements for DAVINCI, and also suggests that oversampling at longer wavelengths does not result in a penalty for SNR.

On the other hand, within the infrared bands the sky background does limit the maximum exposure time before either the accumulated charge rises to the point where the detector's response becomes non-linear or saturates. Here, smaller pixels are better, allowing significantly longer exposure times.

Finally, when the benefit of a larger field of view is considered it seems logical to consider either the 7 or 8 mas pixel scale as the best choice. The 8 mas scale offers shorter exposure times to reach a background limited condition, and also offers a field of view that takes better advantage of the 40" diameter FOV of the AO system. For this reason we have baselined the 8 mas scale. It does have the disadvantage of undersampling the I band, where the Strehl is an average of 15%. Given the relatively broad PSF this undersampling is probably acceptable. However, there is no significant penalty except for a reduction in FOV if the 7 mas scale is adopted instead. This change would have minimal impact on the optical design.



Next Generation Adaptive Optics

## DAVINCI Imager Plate Scales and Sensitivities

December 9, 2009 Revised April 10, 2010

---

### REFERENCES

- Adkins, S. (2009, January 20). Keck Next Generation Adaptive Optics Detectors for NGAO Instrumentation. Keck Adaptive Optics Note 556. Waimea, HI: W. M. Keck Observatory.
- Adkins, S. (2009, September 14). NGAO science instrumentation: Design Concept. Waimea, HI: W. M. Keck Observatory.
- Adkins, S., & McGrath, E. (2010, April 10). DAVINCI background and zero point estimates. Waimea, HI: W. M. Keck Observatory.
- Adkins, S., Larkin, J., Max, C. & McGrath, E. (2009, July 3). NGAO science instrumentation baseline capabilities summary. Waimea, HI: W. M. Keck Observatory.
- Baek, M. & Marchis, F. (2007, November 27). Next Generation Adaptive Optics: Optimum pixel sampling for asteroid companion studies. Keck Adaptive Optics Note 529. Waimea, HI: W. M. Keck Observatory.
- Bauman, B. J. (2009). Anisoplanatism in adaptive optics systems due to pupil aberrations.
- Dekany, R., Neyman, C., Wizinowich, P., McGrath, E. & Max, C. (2009, March 10). Build-to-cost architecture wavefront error performance. Keck Adaptive Optics Note 644. Waimea, HI: W. M. Keck Observatory.
- Hardy, J. W. (1998). *Adaptive optics for astronomical telescopes*. Oxford, UK: Oxford University Press.
- Kulas, K. (2010, January). MOSFIRE detector testing status. Retrieved January 15, 2010 from <http://irlab.astro.ucla.edu/mosfire/team/meetings/meeting63/20100115-MOSFIRE%20Detector-Kulas.ppt>
- Kupke, R. (2009, October 27). NGAO optical relay design. Keck Adaptive Optics Note 685. Santa Cruz, CA: UCO/Lick Observatory.
- Smith, W. J. (2000). *Modern Optical Engineering*. New York, NY: McGraw-Hill.
- Tokunaga, A. T. & Vacca, W. (2005, April). The Mauna Kea Observatories near-infrared filter set. III. Isophotal wavelengths and absolute calibration. *The Publications of the Astronomical Society of the Pacific*, 117(830), 421-426. Chicago, IL: University of Chicago Press.



Next Generation Adaptive Optics

**DAVINCI Imager Plate Scales and Sensitivities**

December 9, 2009 Revised April 10, 2010

---

**APPENDIX**

Passband	Wavelength, nm	$\lambda/D$ (")	$\lambda/D$ (mas)	$\lambda/2D$ (mas)	$\lambda/3D$ (mas)	$\lambda/4D$ (mas)	$\lambda/5D$ (mas)
K band cut-off	2370	0.045	44.7	22.3	14.9	11.2	8.9
K band cut-on	2030	0.038	38.2	19.1	12.7	9.6	7.6
H band cut-off	1780	0.034	33.5	16.8	11.2	8.4	6.7
H band cut-on	1490	0.028	28.1	14.0	9.4	7.0	5.6
J band cut-off	1330	0.025	25.1	12.5	8.4	6.3	5.0
J band cut-on	1170	0.022	22.0	11.0	7.3	5.5	4.4
Y band cut-off	1070	0.020	20.2	10.1	6.7	5.0	4.0
Y band cut-on	970	0.018	18.3	9.1	6.1	4.6	3.7
Z band cut-off	922	0.017	17.4	8.7	5.8	4.3	3.5
Z band cut-on	818	0.015	15.4	7.7	5.1	3.9	3.1
I band cut-off	853	0.016	16.1	8.0	5.4	4.0	3.2
I band cut-on	700	0.013	13.2	6.6	4.4	3.3	2.6

**Table 9: Diffraction limited image size and corresponding pixel scale for 2 to 5 pixel sampling for the six NGAO photometric wavelength bands, the cut-off wavelengths are indicated by gray shading**